3-Phenyl-4-acyl-5-isoxazolonate complex of Tb^{3+} doped into poly-β-hydroxybutyrate matrix as a promising light-conversion molecular device†

Silvanose Biju,[a] M. L. P. Reddy,*[a] Alan H. Cowley[b] and Kalyan V. Vasudevan[b]

Received 16th March 2009, Accepted 18th May 2009
First published as an Advance Article on the web 10th June 2009
DOI: 10.1039/b905304b

A novel class of efficient antenna complexes of Tb^{3+} based on the use of 3-phenyl-4-acyl-5-isoxazolone ligands has been designed, synthesized, characterized and their photophysical properties evaluated . The new heterocyclic β-diketonate complexes of Tb^{3+} exhibit high green luminescence efficiency in the solid state with quantum yields between 59–72%. Furthermore in this work, the synthesis, characterization and luminescent properties of poly-β-hydroxybutyrate (PHB) polymer films doped with Tb^{3+}-3-phenyl-4-acyl-5-isoxazolonate complexes at 5, 10, 15 and 20% (mass) are reported. The fact that the luminescent efficiency of doped films is enhanced (quantum yields between 74–86%) compared with precursor samples revealed that the polymer matrix acts as a co-sensitizer for Tb^{3+}centers. The luminescence intensity decreases, however, with increasing precursor concentration in the doped PHB to greater than 15% where a saturation effect is observed, indicating that changes in the polymer matrix improve the absorption properties of the film, consequently quenching the luminescent effect. Synthesized luminescent polymers containing Tb^{3+}-hetrocyclic β-diketonate complexes showed promising photoluminescence efficiency for applications to polymer light-emitting diodes and active polymer optical fibers.

Introduction

The fascinating optical properties of lanthanide ions have promoted the use of their complexes in an increasing number of technological applications ranging from biomedical analysis to materials science.[1,2] Unfortunately, due to the Laporte forbidden character and intraconfigurational nature of the 4*f* transitions, the molar absorption coefficients of lanthanide transitions are typically very small (less than 10 M^{-1} cm^{-1}). To obviate this problem, organic ligands with large molar absorption coefficients can be coordinated to the lanthanide ion, resulting in sensitized emission by means of the so-called "antenna effect". The β-diketone ligand class is emerging as one of the important "antennas" in terms of high harvest emissions due to the effectiveness of the energy transfer from this ligand type to the Ln^{3+} cation. In part, this is due to the fact that the π–π* transition for β-diketones is intense and occurs over a significant range of wavelengths that is appropriate for sensitization of Ln^{3+} cation luminescence.[3] An additional and practical advantage of the use of β-diketone ligands is that they form stable complexes with Ln^{3+} cations.

It is also worth noting that heterocyclic β-diketones such as 1-phenyl-3-methyl-4-acyl-5-pyrazolones[4] and 3-phenyl-4-benzoyl-5-isoxazolones[5] have also been successfully employed as sensitizers for Eu^{3+} and Tb^{3+}. In a previous report,[5b] it was shown that 3-phenyl-4-aroyl-5-isoxazolones sensitize Tb^{3+} poorly due to possible back transfer of energy from the Tb^{3+} excited state to the $^3\pi$–π^* triplet state of the 3-phenyl-4-benzoyl-5-isoxazolone (HPBI) and 3-phenyl-4-(4-toluoyl)-5-isoxazolone (HTPI) ligands. In turn, this was attributed to the small energy gap between the $^5D_4$ state of the Tb^{3+} cation (20 400 cm^{-1}) and the $^3\pi$–π^* state of the supporting ligands [$\Delta E(^3\pi\pi^*–^5D_4)$ = 1820 cm^{-1} for HPBI and 2220 cm^{-1} for HTPI].[5b] With the twin objectives of increasing this energy gap and developing a robust sensitizer for Tb^{3+}, we have synthesized two new 3-phenyl-4-acyl-5-isoxazolones by introducing aliphatic substituents into the 4-position of the isoxazolone ring, namely 3-phenyl-4-propionyl-5-isoxazolone (HPPI) and 4-isobutyryl-3-phenyl-5-isoxazolone (HIBPI) (Fig. S1 in ESI†). We report (i) the first use of 3-phenyl-4-acyl-5-isoxazolones as sensitizers for Tb^{3+}, and (ii) the isolation and structural authentication of the highly luminescent complexes $Tb(PPI)_3(H_2O)_2$ (**1**) and $Tb(IBPI)_3(C_2H_5OH)$ (H_2O) (**2**). The use of the 3-phenyl-4-acyl-5-isoxazolones as sensitizers for Tb^{3+} results in high quantum yields in the solid state (59 ± 6% and 72 ± 7% for HPPI and HIBPI, respectively). Eu^{3+} complexes [$Eu(PPI)_3(H_2O)_2$ (**3**) and $Eu(IBPI)_3(C_2H_5OH)$ (H_2O) (**4**)] have also been synthesised and their photophysical properties were compared with Tb^{3+} analogues for better understanding of the photosensitization of Ln^{3+} ions.

It has always been a challenging task to synthesize lanthanide complexes with high quantum yields that will also be thermodynamically stable and compatible with advanced microelectronic technologies for thin film production. The growing importance of polymer films in integrated optic technology makes it interesting to investigate the incorporation of lanthanide complexes in a polymer matrix.[6] Although there have been

---

[a] *Chemical Sciences and Technology Division, National Institute for Interdisciplinary Science & Technology (NIIST), Thiruvananthapuram, 695 019, India. E-mail: mlpreddy55@gmail.com*
[b] *Department of Chemistry and Biochemistry, The University of Texas at Austin, 1 University Station A5300, Austin, Texas, 78712, USA*

† Electronic supplementary information (ESI) available: Synthetic protocols and characterisation, experimental details and additional data for photophysical experiments. CCDC reference numbers 703223, 702914 and 703224 for the ligand HIBPI and complexes **1–2**. For ESI and crystallographic data in CIF or other electronic format see DOI: 10.1039/b905304b

several reports on photoluminescence properties of polymer systems doped with Ln^{3+} complexes,[7] studies on the incorporation of Tb^{3+}-3-phenyl-4-acyl-5-isoxazolonate complexes into a polymer matrix are lacking. Hence in the present study, an attempt has also been made to incorporate the highly luminescent Tb^{3+}complexes **1–2** into poly-*β*-hydroxybutyrate (PHB), by replacing the solvent molecules present in the first coordination sphere with the C=O group of PHB. Furthermore, PHB is an environmentally benign material owing to its biodegradable properties which make it an advantageous material as the host structure in luminescent devices.

Results and discussion

Synthesis and characterization of the ligands

The ligands HPPI and HIBPI were synthesized in 80 and 76% yields, respectively, by treatment of 3-phenylisoxazol-5(4*H*)-one with the appropriate acid anhydride using a modification of the literature procedure.[8] The substrate 3-phenylisoxazol-5(4*H*)-one has the possibility of undergoing *C*-acylation at C-4, however such reactions have generally been reported only when acid orthoesters are used.[9] However, Korte and Storiko[8] claimed that they have achieved a C-4 acylated product for 3-phenylisoxazol-5(4*H*)-one by boiling acetic anhydride in the presence of sodium acetate without offering any spectral evidence.[10] Our efforts to synthesize the C-4 acylated products in the above mentioned procedures were not fruitful due to the formation of *N*-acyl derivatives as reported by Prager and co-workers.[10] A detailed study on the relative proportions of acylation products has been investigated and reported that aliphatic acid anhydrides and acid chlorides generally react at nitrogen and aroyl halides give significant proportions of *O*-acylated products.[10] The ligands HPPI and HIBPI were synthesized according to Scheme 1 and the detailed procedure is given in the experimental section. The new ligands were identified by elemental analyses, FT IR, FAB-MS, ^1H NMR and ^{13}C NMR spectral analyses (Fig. S2–S3 in ESI†). The chemical shift of H-4 in the ^1H NMR spectrum was diagnostic: H-4 protons in *N*-acylated compounds are generally detected around *δ* 5.4, and H-4 in *O*-acylated derivatives around *δ* 6.1. Additionally, the infrared spectrum of an *N*-acylated compound would be expected to show a lactone stretching frequency around 1760 cm^{-1}.[10] None of the ligands in the present study shows either an IR stretching band at 1760cm^{-1} or an NMR peak in the region *δ* 5–7. The existence of the ligands in the enolic form was confirmed by single-crystal X-ray diffraction analysis (Fig. S1c in ESI†).

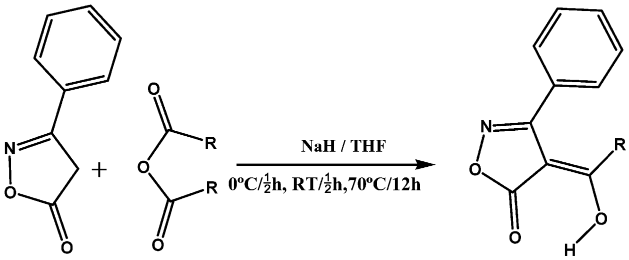

R= C_2H_5, HPPI and R = $CH(CH_3)_2$, HIBPI

Scheme 1 Synthesis procedure for the ligands.

Synthesis and characterization of the complexes 1–6

The procedure employed for the syntheses of Ln^{3+} complexes **1–6** is shown in Scheme 2. The elemental analyses and FAB-MS studies of complexes **1–6** reveal that each Ln^{3+} ion has reacted with the *β*-diketones in a metal-to-ligand mole ratio of 3:1 and that two solvent molecules are incorporated in the coordination sphere. Powder X-ray diffraction studies (Fig. S4 in ESI†) showed that complexes **1–6** are isostructural. The carbonyl stretching frequency of HPPI and HIBPI (1704 cm^{-1}) is shifted to lower wave numbers in complexes **1–6** (1648 cm^{-1} in **1**; 1642 cm^{-1} in **2**; 1648 cm^{-1} in **3**; 1645 cm^{-1} in **4**; 1650 cm^{-1} in **5**; 1658 cm^{-1} in **6**), indicating the involvement of carbonyl oxygen in the complex formation with the Ln^{3+} ion. The appearance of a broad band (3000–3500 cm^{-1}) in the IR spectra of complexes **1–6** reveals the presence of coordinated solvent molecules in the corresponding complexes. The presence of solvent molecules in these complexes has been further confirmed by the fact that all of these complexes exhibit mass loss at around 150 °C corresponding to the removal of solvent molecules during thermogravimetric analysis (Fig. S5 in ESI†). Subsequent thermal decomposition of **1–6** takes place in two steps in the temperature region 240–600 °C. The residue for each complex is approximately 20% of the initial mass which corresponds to the respective lanthanide oxide.

Structural insights of the complexes **1–2** were provided by single-crystal X-ray studies. Crystal data, collection, and structure refinement parameters for the complexes **1–2** are presented in Table 1 and selected bond lengths and angles in Table 2. Both

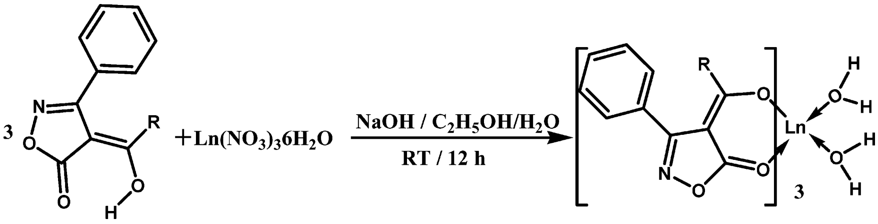

Ln = Tb and R = C_2H_5, (1), $CH(CH_3)_2$ (2)

Ln = Eu and R = C_2H_5, (3), $CH(CH_3)_2$ (4)

Ln = Gd and R = C_2H_5, (5), $CH(CH_3)_2$ (6)

Scheme 2 Synthesis procedure for complexes **1–6**.

Table 1 Crystal data, collection, and structure refinement parameters for the ligand HIBPI and complexes **1–2**

Parameters	HIBPI	1	2
Empirical formula	$C_{13}H_{13}NO_3$	$C_{36}H_{34}N_3O_{11}Tb$	$C_{41}H_{44}N_3O_{11}Tb$
fw	231.24	843.58	913.71
Crystal system	Orthorhombic	Monoclinic	Monoclinic
Space group	P*bca*	$P2_1/c$	$P2_1/c$
Cryst size (mm^3)	0.3 × 0.2 × 0.2	0.13 × 0.12 × 0.10	0.3 × 0.2 × 0.2
Temperature (K)	293(2)	153(2)	293(2)
a/Å	16.244(5)	22.803(5)	8.756(5)
b/Å	8.813(5)	5.9919(12)	38.268(5)
c/Å	16.888(5)	26.097(5	12.162(5)
α (deg)	90	90	90
β (deg)	90	101.27(3)	96.327(5)
γ (deg)	90	90	90
V/Å^3	2417.7(17)	3496.9(12)	4050.4(3)
Z	8	4	4
ρ_{calcd}/g cm^{-3}	1.271	1.602	1.498
μ/mm^{-1}	0.091	2.088	1.809
F(000)	976	1696	1856
R1 [$I > 2\sigma(I)$]	0.0427	0.0466	0.0512
wR2 [$I > 2\sigma(I)$]	0.1112	0.0999	0.1125
R1 (all data)	0.0864	0.0886	0.0816
wR2 (all data)	0.1269	0.1282	0.1271
GOF	0.965	1.052	1.197

Table 2 Selected bond lengths [Å] and angles [°] for complexes **1** and **2**

1		2	
Tb–O(1)	2.358(4)	Tb–O(1)	2.367(2)
Tb–O(2)	2.369(4)	Tb–O(2)	2.348(3)
Tb–O(3)	2.363(4)	Tb–O(4)	2.371(2)
Tb–O(4)	2.399(4)	Tb–O(5)	2.319(2)
Tb–O(5)	2.358(4)	Tb–O(7)	2.329(2)
Tb–O(6)	2.386(4)	Tb–O(8)	2.337(3)
Tb–O(10)	2.415(4)	Tb–O(10)	2.419(3)
Tb–O(11)	2.373(4)	Tb–O(11)	2.463(3)
O(1)–Tb–O(2)	73.07(13)	O(1)–Tb–O(2)	72.32(8)
O(3)–Tb–O(4)	72.81(12)	O(4)–Tb–O(5)	74.66(8)
O(5)–Tb–O(6)	74.19(13)	O(7)–Tb–O(8)	73.66(9)
O(10)–Tb–O(11)	144.64(13)	O(10)–Tb–O(11)	75.05(10)

complexes crystallize in the monoclinic space group $P2_1/c$ with Z = 4. There are no unusually short intermolecular contacts in either structure. Each complex is eight-coordinate and the coordination sphere features three bidentate PPI or IBPI ligands and two solvent molecules (Fig. 1 and 2). In the case of **1**, these are both water molecules, while in the case of **2** there is one water and one ethanol molecule. The coordination geometries of both complexes are best described as bicapped trigonal prismatic. The average bond distance between the Tb^{3+} cation and the isoxazolone oxygen atoms is some what shorter for **2** (2.344(8) Å) than for **1** (2.372(4) Å) which suggests that the HIBPI ligand binds slightly more strongly to Tb^{3+} than the HPPI analogue. For both **1** and **2**, the metal-oxygen distances are shorter for the isoxazolone ligands than for the solvent molecules. The latter observation could be attributed to the presence of a formal negative charge on the isoxazolone oxygen atoms which could enhance the binding to the Tb^{3+} cation due to electrostatic effects.[5]

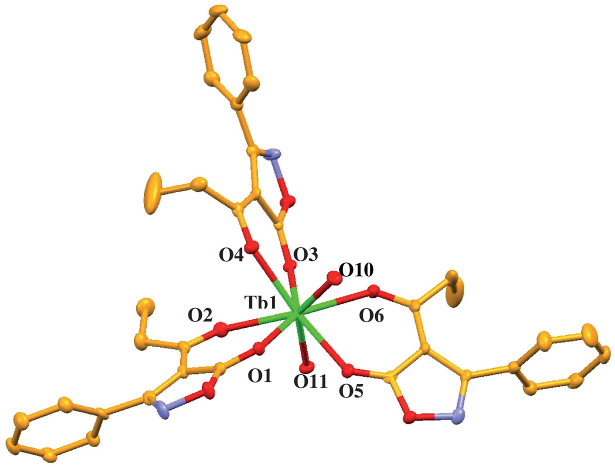

Fig. 1 Asymmetric unit of complexes **1**, thermal ellipsoids drawn with 30% probability and hydrogen atoms omitted for clarity.

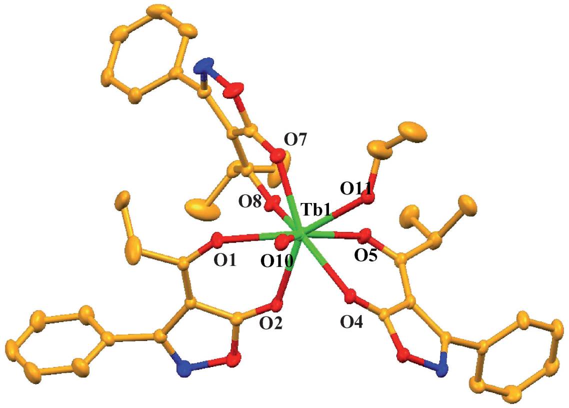

Fig. 2 Asymmetric unit of complexes **2**, thermal ellipsoids drawn with 30% probability and hydrogen atoms omitted for clarity.

Steady-state photoluminescence of 1–2

It is clear both from the excitation spectra of complexes **1** and **2** and also from the absorption spectra of the ligands (Fig. S6 in ESI†) that overlap exists between the excitation band of each Tb^{3+} complex and the absorption bands of the ligands. Such an observation is typically diagnostic of ligand sensitization of a lanthanide cation[11] and therefore confirms that the HPPI and HIBPI ligands are coordinated to the Tb^{3+} cation in **1** and **2**, respectively.[12] The excitation spectra (Fig. 3) for both **1** and **2** exhibit a broad band between 250 and 350 nm which is attributable to the π–π* transition of the heterocyclic β-diketone ligand. A series of sharp lines that are assignable to transitions between the lanthanide $^7F_5$ and $^5G_6$, $^5L_{10}$ and $^5L_9$ levels are also observed in the excitation spectra of both complexes. The latter transitions are less intense than the absorptions due to the organic ligands and are overlapped by a broad excitation band. In turn, this proves that luminescence sensitization *via* excitation of the ligand is considerably more efficient than the direct excitation of the Tb^{3+} absorption level.

The room-temperature emission spectra of complexes **1** and **2** (Fig. 3) exhibit the characteristic emission bands of the Tb^{3+}

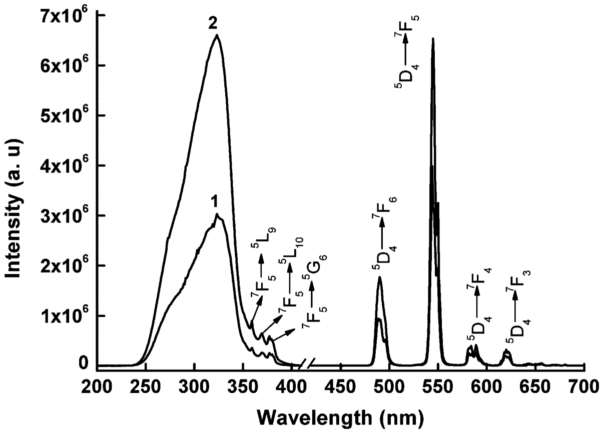

Fig. 3 Solid state excitation and emission spectra for complexes **1** and **2** at 298 K (λ_{ex} 320 nm and emission monitored at 545 nm).

cation (λ_{ex} 320 nm) centered at 488, 545, 585, and 620 nm which result from deactivation of the $^5D_4$ excited state to the corresponding ^7F_J ground state of the Tb^{3+} cation (J = 6,5,4,3). The most intense emission is centered at 545 nm and corresponds to the $^5D_4 \rightarrow {}^7F_5$ transition.[4c,5b] Fig. S7 in ESI† illustrates the room-temperature excitation and emission spectra of the Eu^{3+} complexes **3–4**. It is clear from the excitation spectra of **3–4** that Eu^{3+} absorption peaks are dominating the ligand centered excitation band. Thus it can be concluded that HPPI and HIBPI ligands are not efficient sensitizers for Eu^{3+}.

The overall quantum yield ($\Phi_{overall}$) for a lanthanide complex treats the system as a "black box" in which the internal process is not considered explicitly. Given that the complex absorbs a photon (*i.e.* the antenna is excited), the overall quantum yield can be defined as follows:[13]

$$\Phi_{overall} = \Phi_{sen}\Phi_{Ln} \tag{1}$$

Here, Φ_{sen} represents the efficiency of energy transfer from the ligand to the Ln^{3+} ion and Φ_{Ln} represents the intrinsic quantum yield of the Ln^{3+} ion, which can be calculated as

$$\Phi_{Ln} = \left(\frac{A_{RAD}}{A_{RAD} + A_{NR}}\right) = \frac{\tau_{obs}}{\tau_{RAD}} \tag{2}$$

For the Eu^{3+} complexes, the radiative lifetime (τ_{RAD}) can be calculated using Equation (3),[14,3c] assuming that the energy of the $^5D_0 \rightarrow {}^7F_1$ transition (MD) and its oscillator strength are constant

$$A_{RAD} = \frac{1}{\tau_{RAD}} = A_{MD,0}n^3\left(\frac{I_{TOT}}{I_{MD}}\right) \tag{3}$$

where $A_{MD,0}$ (14.65 s^{-1}) is the spontaneous emission probability of the $^5D_0 \rightarrow {}^7F_1$ transition in vacuo, I_{TOT}/I_{MD} is the ratio of the total area of the corrected Eu^{3+} emission spectrum to the area of the $^5D_0 \rightarrow {}^7F_1$ band and n is the refractive index of the medium. An average index of refraction equal to 1.5 was considered.[5a] The intrinsic quantum yield of Tb^{3+} (Φ_{Tb}) can be estimated through Equation (4) by using the assumption that the decay process at 77 K in deuterated solvent is purely radiative.[11a,15]

$$\Phi_{Tb} = \frac{\tau_{obs\,(298\mathrm{K})}}{\tau_{RAD\,(77\mathrm{K})}} \tag{4}$$

Quantum yields (Table 3) of the complexes in the solid state were determined according to the absolute method of Wrighton.[16] The quantum yields of the Tb^{3+}complexes were found to be unexpectedly high (59 ± 6% for **1** and 72 ± 7% for **2**; λ_{exc} = 320 nm), which is surprising in view of the presence of C_2H_5OH and H_2O molecules in the first coordination sphere, as they are usually both essential vibrational deactivators of the excited states of Ln^{3+} ions. However, similar high quantum yields (88%) have been observed previously for Tb^{3+}-*p*-aminobenzoates in the presence of H_2O molecules.[17] The energy gap between the luminescent state and the ground state manifold is approximately 12000 cm^{-1} for Eu^{3+} and 14800 cm^{-1} for Tb^{3+}.[18] Relatively efficient coupling of the Eu^{3+} excited states occurs to the third vibrational overtone of proximate OH oscillators ($\nu_{OH} \sim$ 3300–3500 cm^{-1}), and to the fourth harmonic in the case of Tb^{3+}, consistent with the observed less efficient quenching for Tb^{3+}, where the Franck–Condon overlap factor is less favourable.[18] The obtained quantum yield values of Tb^{3+}-3-phenyl-4-acyl-isoxazolonates are found to be significantly higher than those reported for Tb^{3+} hexafluoroacetylacetonate and dipivaloylmethanato complexes ($\Phi_{overall}$ = 27 and 40%, respectively).[19] On the other hand, poor quantum yields for the Eu^{3+} complexes have been noticed.

The $^5D_4$ lifetime of the green emission of Tb^{3+} complexes was determined by single-exponential fitting of the decay curve (Fig. S8–S11 in ESI†) and is consistent with the presence of one major luminescent species. The pertinent lifetime values are 785 ± 2 and 920 ± 3 μs for **1** and **2**, respectively. Again it is surprising to note that the magnitude of the $^5D_4$ lifetime values of these complexes is not very high as compared to some of the recently reported highly luminescent complexes of Tb^{3+} ($\Phi_{overall}$ = 56%; τ_{obs} = 2.63 ms).[20] However, there are reports with $\Phi_{overall}$ = 40% and τ_{obs} = 0.46 ms for Tb^{3+}-dipivaloylmethanato complexes.[19] The lifetime is the inverse of the total de-activation rate, itself the sum of the radiative and non-radiative rates. Therefore a complex may be highly luminescent and have a short lifetime, there is no contradiction. It simply means that the radiative rate

Table 3 Photophysical data for Tb^{3+} and Eu^{3+} complexes

Complex	ΔE ($^3\pi\pi^*$ – ^5D_J) [cm^{-1}]	τ_{RAD} [μs]	τ_{obs} [μs]	Φ_{Ln} [%]	Φ_{sen} [%]	$\Phi_{overall}$ [%][a]
1	3240	807	785 ± 2	97	61	59 ± 6
2	2750	961	920 ± 3	96	75	72 ± 7
3	6390	1700	259 ± 1	15	2	0.3 ± 0.03
4	5300	1650	261 ± 1	16	3	0.5 ± 0.05

[a] Average value of three measurements performed under the same experimental conditions.

is fast as observed in the present Tb^{3+}complexes. Due to its electronic structure, Tb^{3+} has many levels which can mix with ligand wave functions, including a relatively low-lying $4f\,5d$ state, which may explain why the lifetime is relatively short (*i.e.* it means that the phosphorescence character of the transition is partly lost). The relatively shorter $^5D_0$ lifetime values of Eu^{3+} analogues (Fig. S12–S13 in ESI†) observed may be due to the dominant non-radiative decay channels associated with vibronic coupling because of the presence of solvent molecules, also documented in many of the hydrated europium β-diketonate complexes.[3c,5a] The radiative lifetimes (τ_{RAD}), intrinsic quantum yields (Φ_{Ln}), and sensitization efficiency (Φ_{sen}) values of the ligands in Ln^{3+} complexes **1–4** were calculated and are given in Table 3.

In order to elucidate the energy transfer process in **1** and **2**, it was necessary to determine the energy levels of the relevant electronic states of the ligands. The singlet ($^1\pi\pi^*$) and triplet ($^3\pi\pi^*$) energy levels of the HPPI and HIBPI ligands were estimated by reference to the wavelengths of the UV-Vis absorption edges of **1** an **2** (320 nm: 31250 cm^{-1} and 321 nm: 31150 cm^{-1} for HPPI and HIBPI, respectively: Fig. S6 in ESI†) and the lower wavelength emission edges (423 nm: 23640 cm^{-1} and 432 nm: 23150 cm^{-1} for HPPI and HIBPI, respectively) for the corresponding phosphorescence spectra of the gadolinium complexes $Gd(PPI)_3(H_2O)_2$ **5** and $Gd(IBPI)_3(H_2O)_2$ **6** (Fig. S14 in ESI†). It can be seen from Fig. S14 in ESI† that there exists a large area of overlap between the room-temperature emission spectra of the ligands and the low-temperature phosphorescence spectra of complexes **5–6**. Furthermore, it is also evident that there is an overlap between the low-temperature phosphorescence spectra of complexes **5–6** and the emission spectra of the Ln^{3+} complexes. The above spectral overlap clearly indicates the sensitization pathway in luminescent Ln^{3+} complexes consists of excitation of the coordinated ligands into their excited states, subsequent intersystem crossing of the ligands to their triplet states and energy transfer from the triplet state of the ligand to the ^5D_J manifold of the Ln^{3+} ion. This is followed by internal conversion to the emitting state of the Ln^{3+}, and finally the Ln^{3+} ion emits radiation. Therefore, the energy-level match between the triplet states of the ligands to the ^5D_J state of the Ln^{3+} cation is one of the key factors that govern the luminescence properties of Ln^{3+} complexes. According to Reinhoudt's empirical rule,[21] the intersystem crossing process will be effective when $\Delta E(^1\pi\pi^*–^3\pi\pi^*)$ is approximately 5000 cm^{-1}. It has been observed that the $\Delta E(^1\pi\pi^*–^3\pi\pi^*)$ energy gaps for HPPI and HIBPI are 7610 and 8000 cm^{-1}, respectively and hence the intersystem crossing processes are effective for both the ligands. Latva's empirical rule[22] states that an optimal ligand-to-metal energy transfer process for Ln^{3+} needs ΔE ($^3\pi\pi^*–^5D_J$) = 2500–4000 cm^{-1} for $Eu^{3+}$and 2500–4500 cm^{-1} for Tb^{3+}. On this basis it can be concluded that the energy transfer to the Tb^{3+} cation will be effective for the HPPI and HIBPI ligands since $\Delta E(^3\pi\pi^*–^5D_4)$ for **1** and **2** are 3240 and 2750 cm^{-1}, respectively. Complex **2** exhibits a higher luminescence efficiency than complex **1** due to a superior match of the triplet energy level with that of the Tb^{3+} emitting level. On the other hand, poor sensitization for Eu^{3+} has been noted for the above chromophores mainly due to the larger energy gap between the ligand triplet state and $^5D_0$ level of Eu^{3+} $\Delta E(^3\pi\pi^*–^5D_0)$ = 6390 cm^{-1} for **3** and 5900 cm^{-1} for **4**. This therefore supports the observation of stronger sensitization of the Tb^{3+} complexes (Φ_{sen} = 61–75%) than the Eu^{3+} complexes (Φ_{sen} = 2–3%) because of the smaller overlap between the ligand triplet and Eu^{3+} ion excited states than that of Tb^{3+} (Fig. S14 in ESI†). A schematic diagram representing all of the possible energy transfer pathways for complexes **1–4** is depicted in Fig. S15 (ESI†).

Photophysical properties of Tb^{3+} complexes doped PHB polymer films

Inspired by the excellent luminescent efficiency of the Tb^{3+}complexes **1–2**, the authors incorporated these complexes into a polymer matrix, namely poly-β-hydroxybutyrate (PHB), by replacing the solvent molecules present in the first coordination sphere with the C=O group of PHB. A schematic representation of the Tb^{3+} complex coordinated to the PHB polymer film backbone is shown in Fig. 4. The PHB polymer was doped with the Tb^{3+} complexes **1–2** in the proportions of 5, 10, 15 and 20% (w/w). The broad absorption band assigned to the H_2O vibrational modes in the FTIR spectra of the precursor Tb^{3+} complexes identified in the region (3000–3500 cm^{-1}) is absent for the doped PHB polymer films confirming that the polymer films

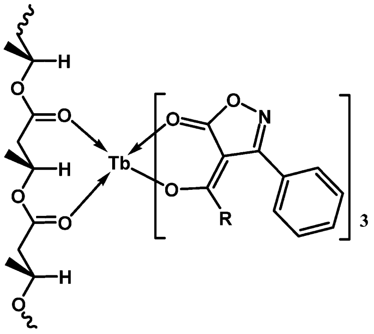

R = C_2H_5 (**1**), $CH(CH_3)_2$ (**2**)

Fig. 4 A schematic representation of the structure of Tb^{3+} complex doped in PHB polymer.

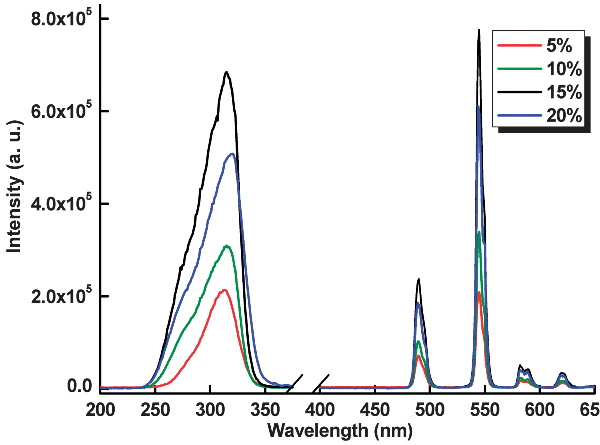

Fig. 5 Excitation and emission spectra of PHB: 5–20% $Tb(PPI)_3$ polymer film systems recorded at 298 K (excited at 320 nm and emission monitored at 545 nm).

are anhydrous. This is again in good agreement with the TG analyses of doped polymer films, where no mass loss was noted in the temperature region 50–200 °C (Fig. S16 in ESI†). The typical thermogravimetric analyses of the PHB polymer film and Tb^{3+} complexes doped with PHB polymer at a ratio of 15% (w/w) were recorded under inert atmosphere of nitrogen and the results are illustrated in Fig. S16 (ESI†). It is clear from the thermogravimetric curve that the un-doped polymer film decomposes in a one step event and its decomposition starts at 260 °C. Similarly, the Tb^{3+} complex doped polymer films also decompose in a single step event under an inert atmosphere. However, the doped polymer films exhibit decreasing onset temperatures of decomposition of 230 and 231 °C for **1–2**, respectively.

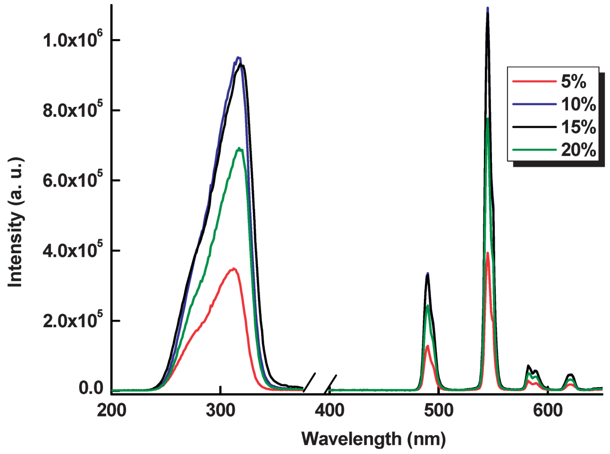

Fig. 6 Excitation and emission spectra of PHB: 5–20% $Tb(IBPI)_3$ polymer film systems recorded at 298 K (excited at 320 nm and emission monitored at 545 nm).

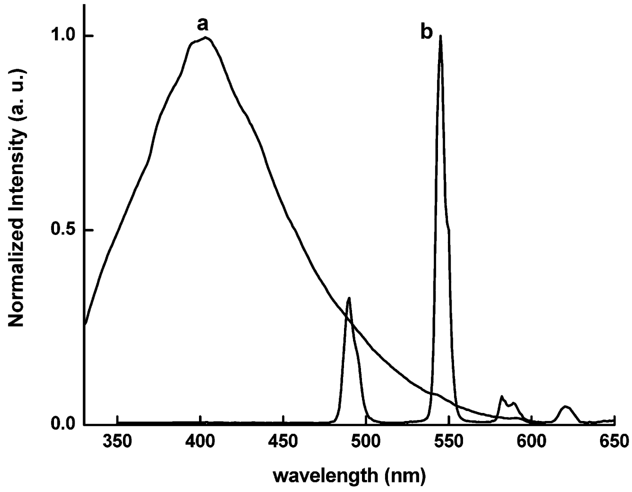

Fig. 7 Emission spectra recorded at 298 K, under excitation monitored at 320 nm: (a) undoped PHB film and (b) PHB:15% $Tb(IBPI)_3$ film.

The excitation spectra of the PHB polymer films doped with the Tb^{3+} complexes (**1–2**) at different doping concentrations (5, 10, 15 and 20% w/w) recorded at 298K in the spectral range 200–400 nm, by monitoring the emission at 545 nm, are given in Fig. 5 and 6. These excitation spectra exhibit an intense broad band in the spectral region 250–350 nm, which can be assigned to both PHB polymer and organic chromophore absorptions. Furthermore, the typical intraconfigurational transitions pertaining to Tb^{3+} ion noted in the precursor samples are absent in these excitation spectra, owing to the efficient energy transfer from both organic moiety and polymer matrix to the central metal ion. These facts suggest that polymer matrices serve as efficient co-sensitizers for the Tb^{3+} ions.

The emission spectra of the un-doped PHB polymer and PHB:15% $Tb(IBPI)_3$ films recorded at 298 K in the range from 330–650 nm under excitation at 320 nm are depicted in Fig. 7. The absence of a broad polymer emission band in the doped film indicates highly efficient energy transfer *via* the polymer matrix to the Tb^{3+} ion. As shown in Fig. 5 and 6, the luminescent intensity of the Tb^{3+} emission at 545 nm increases with increasing Tb^{3+} content and reaches a maximum at the Tb^{3+} content of 15%. A further increase of the Tb^{3+} content decreases the luminescent intensity of the Tb^{3+}emission. The energy transfer between the lanthanide ions themselves is a nonradiative process, which would account for the decrease of the Tb^{3+} emission, especially at high Tb^{3+} content.[5d,23]

The luminescent peaks of the Tb^{3+} complexes with and without the presence of PHB do not display noticeable shifts in the positions. However, some transitions show variations in intensity that depends strongly on the coordinative environment, as shown in Fig. 5 and 6. It is well documented that for Tb^{3+}complexes the magnetic dipole transition $^5D_4 \rightarrow {}^7F_5$ is largely independent of the ligand field and therefore can be used as an internal standard to account for the ligand differences.[19,24] The electric dipole transition $^5D_4 \rightarrow {}^7F_6$, a so-called hypersensitive transition,[19,24] is sensitive to the symmetry of the coordination sphere. The intensity ratio of the electric dipole transition to the magnetic dipole transition in the lanthanide complex measures the symmetry of the coordination sphere[25,26] and this ratio increases with the number and mass of the ligand coordinated by

Table 4 Integral corrected intensities of the $^5D_4 \rightarrow {}^7F_J$ relative to the $^5D_4 \rightarrow {}^7F_5$ transitions, $\Phi_{overall}$ and τ_{obs} for Tb^{3+} complex **1**, and PHB:5–20% $Tb(PPI)_3$ polymer film systems upon ligand excitation at 298 K

Complex	$\int_{4-6}$	$\int_{4-5}$	$\int_{4-4}$	$\int_{4-3}$	τ_{obs} [µs][a]	$\Phi_{overall}$ [%][a]
1	0.35	1	0.11	0.06	785 ± 2	59 ± 6
PHB:5% **1**	0.43	1	0.15	0.10	765 ± 5	68 ± 7
PHB:10% **1**	0.40	1	0.12	0.08	795 ± 4	71 ± 7
PHB:15% **1**	0.40	1	0.11	0.06	780 ± 3	74 ± 7
PHB:20% **1**	0.39	1	0.11	0.06	745 ± 2	61 ± 6

[a] Average value of three measurements performed under the same experimental conditions.

Table 5 Integral corrected intensities of the $^5D_4 \rightarrow {}^7F_J$ relative to the $^5D_4 \rightarrow {}^7F_5$ transitions, $\Phi_{overall}$ and τ_{obs} for Tb^{3+} complex **2**, and PHB:5–20% Tb(IBPI)$_3$ polymer film systems upon ligand excitation at 298 K

Complex	$\int_{4-6}$	$\int_{4-5}$	$\int_{4-4}$	$\int_{4-3}$	τ_{obs} [μs]^a	$\Phi_{overall}$ [%]^a
2	0.36	1	0.11	0.06	920 ± 3	72 ± 7
PHB:5% **2**	0.40	1	0.12	0.07	931 ± 2	79 ± 8
PHB:10% **2**	0.41	1	0.10	0.06	922 ± 5	83 ± 8
PHB:15% **2**	0.41	1	0.11	0.06	929 ± 3	86 ± 9
PHB:20% **2**	0.40	1	0.11	0.06	904 ± 5	75 ± 8

^{a} Average value of three measurements performed under the same experimental conditions.

the Ln^{3+} ion.[27] For the Tb^{3+} complex **1** in the absence of PHB, the intensity ratio of the transitions of $^5D_4 \rightarrow {}^7F_6$ to $^5D_4 \rightarrow {}^7F_5$ was 0.35. It increases to 0.39–0.43 (Table 4) for the complex incorporated into the PHB matrix. Similarly, for the Tb^{3+} complex **2** the intensity ratio of the transitions of $^5D_4 \rightarrow {}^7F_6$ to $^5D_4 \rightarrow {}^7F_5$ increases from 0.36 to 0.40–0.41 (Table 5). In short, the presence of PHB generally increases the luminescent intensity of the hypersensitive transitions of the Tb^{3+} ion. For the complexes **1–2** without the capping of PHB, the surrounding environment is less disturbed and the relative intensity of the electric dipole transition $^5D_4 \rightarrow {}^7F_6$ is relatively weak. When incorporated into microcavities of the PHB matrix however, the complexes exhibit disorder of a certain magnitude. Under the influence of the electric field of the surrounding ligands, the distortion of the symmetry around the lanthanide ion by the capping PHB results in the polarization of the Tb^{3+}, which increases the probability for the electric dipole allowed transition. The influence of PHB on the coordination environment of the Tb^{3+} ions changes the energy-transfer probabilities of the electric dipole transitions, accounting for the increases in luminescent intensity of the 488 nm peak. Therefore the overall quantum yields of Tb^{3+} doped PHB films have been enhanced as compared to the precursor samples (Tables 4 and 5).

Experimental details

Materials

The following chemicals were acquired commercially and used without subsequent purification: terbium(III) nitrate hexahydrate, 99.9% (Acros Organics); 3-phenyl -5-isoxazolone, 97% (Aldrich); propanoic anhydride, 97% (Aldrich); isobutric anhydride, 97% (Aldrich) and poly(3-hydroxybutyric acid), natural origin (Aldrich). All the other chemicals used were of analytical reagent grade.

Synthesis of the ligands

The ligands HPPI and HIBPI were synthesized according to Scheme 1. 3-Phenyl-5-isoxazolone (6 mmol) was dissolved in 20 mL of dry THF and stirred for 10 min at 0 °C in an ice bath. To this solution, sodium hydride (12 mmol) was added in an inert atmosphere, followed by the corresponding acid anhydride (12 mmol) then stirred at 0 °C for 30 min, room temperature for 30 min followed by further stirring at 70 °C for 12h. The resulting pale yellow paste was decomposed by adding 2 M HCl (50 mL), and the solution was extracted twice with dichloromethane (70 mL). The organic layer was separated and treated with a saturated solution of $NaHCO_3$. The products were precipitated from the collected aqueous layer using 4 M HCl. The new ligands were identified by elemental analyses and FT IR, FAB-MS, ^1H NMR and ^{13}C NMR spectral data (Fig. S2–S3†). Single crystals of the ligand HIBPI were obtained from a saturated solution of the compound in ethyl acetate after storage for one month.

HPPI. Yield = 80%, mp = 76 ± 2 °C. ^1H NMR (500 MHz, $CDCl_3$, TMS) ppm: 7.46–7.49 (m, 5H), 2.33–2.377 (q, 2H), 1.10–1.13 (t, 3H). ^{13}C NMR (500 MHz, $CDCl_3$, TMS) ppm: 188.00, 177.06, 161.22, 130.72–128.50, 97.28, 77.25–76.75 ($CDCl_3$), 27.07, 10.00. IR (KBr) ν_{max}: 3052, 1704, 1608, 1364, 1200, 848, 698 cm^{-1}. m/z = 218.50 $(M + 1)^+$. CHN anal. calcd for $C_{12}H_{11}NO_3$: C, 66.35; H, 5.10; N, 6.45. Found: C, 66.12; H, 5.37; N, 6.65%.

HIBPI. Yield = 76%, mp = 137 ± 2 °C. ^1H NMR (500 MHz, $CDCl_3$, TMS) ppm: 7.52–7.47 (m, 5H), 2.71–2.63 (m, 1H), 1.13–1.11 (d, 6H). ^{13}C NMR (500 MHz, $CDCl_3$, TMS) ppm: 191.44, 177.31, 161.11, 130.69–128.35, 96.25, 77.26–76.75 ($CDCl_3$), 31.79, 19.15. IR (KBr) ν_{max}: 3050, 1704, 1610, 1366, 1202, 842, 700 cm^{-1}. m/z = 232.46 $(M + 1)^+$. CHN anal. calcd for $C_{13}H_{13}NO_3$: C, 67.52; H, 5.67; N, 6.06. Found: C, 67.74; H, 5.77; N, 6.27%.

Synthesis of the Ln^{3+} complexes

Complexes **1–6** were synthesized by means of the following general procedure.[5] 1 mmol of the appropriate lanthanide nitrate in 2 mL of ethanol was added to a solution of 3 mmol of the ligand and 3 mmol of NaOH in 50 mL of ethanol along with 50 mL of water. The reaction mixture was stirred at room temperature for 12 h. The precipitate thus obtained was filtered off, washed with water and dried in vacuo. Single crystals of complexes **1** and **2** suitable for X-ray diffraction experiments were obtained from an ethanol/dichloromethane (1:1) solution kept in a sealed flask at room temperature for two weeks. These were used for further analyses and the photophysical studies.

$Tb(PPI)_3(H_2O)_2$ (1). Elemental analysis (%): calcd for $C_{36}H_{34}TbN_3O_{11}$ (843.59): C, 51.26; H, 4.06; N, 4.98. Found: C, 51.11; H, 4.06; N, 5.00. IR (KBr) λ_{max}: 3300, 1648, 1496, 1394, 936, 764, 968 cm^{-1}; m/z = 808.13 $[Tb(PPI)_3] + 1$.

$Tb(IBPI)_3(C_2H_5OH)(H_2O)$ (2). Elemental analysis (%): calcd for $C_{41}H_{44}TbN_3O_{11}$ (913.73):C, 53.89; H, 4.85; N, 4.60. Found:

C, 53.64; H, 4.95; N, 4.86. IR (KBr) λ_{max}: 3292, 1642, 1496, 1394, 962, 770 cm^{-1}; *m*/*z* = 836.16 [Tb(IBPI)$_3$] + 1.

$Eu(PPI)_3(H_2O)_2$ (3). Elemental analysis (%): calcd for $C_{36}H_{34}EuN_3O_{11}$ (836.63): C, 51.68; H, 4.10; N, 5.02. Found: C, 51.51; H, 4.09; N, 4.96. IR (KBr) λ_{max}: 3310, 1648, 1496, 1392, 935, 766, 969 cm^{-1}; *m*/*z* = 802.12 [Eu(PPI)$_3$] + 1.

$Eu(IBPI)_3(C_2H_5OH)(H_2O)$ (4). Elemental analysis (%): calcd for $C_{41}H_{44}EuN_3O_{11}$ (906.76):C, 54.31; H, 4.89; N, 4.63. Found: C, 54.60; H, 4.95; N, 4.78 IR (KBr) λ_{max}: 3322, 1645, 1494, 1394, 962, 772 cm^{-1}; *m*/*z* = 829.66 [Eu(IBPI)$_3$] + 1.

$Gd(PPI)_3(H_2O)_2$ (5). Elemental analysis (%): calcd for $C_{36}H_{34}GdN_3O_{11}$ (841.92): C, 51.36; H, 4.07; N, 4.99. Found: C, 50.99; H, 4.11; N, 4.85. IR (KBr) λmax: 3300, 1650, 1494, 1394, 936, 764, 700, cm^{-1}; *m*/*z* = 806.90 [Gd(PPI)$_3$] + 1.

$Gd(IBPI)_3(H_2O)_2$ (6). Elemental analysis (%): calcd for $C_{39}H_{40}GdN_3O_{11}$ (884.00): C, 52.99; H, 4.56; N, 4.75. Found: C, 53.06; H, 4.76; N, 4.69. IR (KBr) λ_{max}: 3428, 1658, 1390, 964, 766, 702 cm^{-1}; *m*/*z* = 835.16 [Gd(IBPI)$_3$] + 1.

Synthesis of Tb^{3+} complex doped PHB polymer films

The PHB polymer was doped with the Tb^{3+} complexes **1–2** in the proportions 5, 10, 15 and 20% (w/w). The PHB powder was dissolved in chloroform followed by addition of the required amount of the Tb^{3+}complex in chloroform/ethanol solution. The mixed solution was heated at 40 °C for 30 min. The polymer film was obtained after the evaporation of excess solvent at 60 °C.[7b]

Characterization

Elemental analyses were performed with a Perkin-Elmer Series 2 Elemental Analyzer 2400. A Perkin-Elmer Spectrum One FT-IR Spectrometer using KBr (neat) was used to obtain the IR spectral data and a Bruker 500 MHz NMR spectrometer was used to record the ^1H NMR and ^{13}C NMR spectra of the new compounds in $CDCl_3$ solution. The mass spectra were recorded on a JEOL JSM 600 fast atom bombardment (FAB) high resolution mass spectrometer (FAB-MS) and the thermogravimetric analyses were performed on a TGA-50H instrument (Shimadzu, Japan). X-Ray powder diffraction (XRD) analyses were performed with a Philips X'Pert Pro diffractometer. The XRD patterns were recorded in the 2θ range 10–70° using Ni filtered Cu Kα radiation. The absorbances of the ligands were measured in CH_3CN solution on a UV-vis spectrophotometer (Shimadzu, UV-2450) and the photoluminescence (PL) spectra were recorded on a Spex-Fluorolog FL22 spectrofluorometer equipped with a double grating 0.22m Spex 1680 monochromator and a 450W Xe lamp as the excitation source operating in the front face mode. The lifetime measurements were carried out at room temperature using a Spex 1040 D phosphorimeter.

The overall quantum yields ($\Phi_{overall}$) were measured using an integrating sphere in a SPEX Fluorolog spectrofluorimeter. The PL quantum yields in thin films ($\Phi_{overall}$) were determined using a calibrated integrating sphere system. The Xe-arc lamp was used to excite the thin-film samples placed in the sphere with 320 nm as the excitation wavelength. Samples were prepared by drop casting the material placed between two quartz cover slips, The quantum yield was determined by comparing the spectral intensities of the lamp and the sample emission as reported in the literature.[28] Using this experimental setup and the integrating sphere system, the solid-state fluorescence quantum yield of thin film of the standard green OLED material tris-8-hydroxyquinolinolato aluminium (Alq_3) was determined to be 0.19, which is consistent with previously reported values.[29] Each sample was measured several times under slightly different experimental conditions. The estimated error for quantum yields is ±10%.[19]

Crystallographic characterization

The X-ray diffraction data were collected at 153 K on a Nonius Kappa CCD diffractometer equipped with an Oxford Cryostream low-temperature device and a graphite-monochromated Mo Kα radiation source (λ = 0.71073 Å). Corrections were applied for Lorentz and polarization effects. All of the structures were solved by direct methods[30] and refined by full-matrix least-squares cycles on F^2. All of the non-hydrogen atoms were allowed anisotropic thermal motion, and the hydrogen atoms were placed in fixed, calculated positions using a riding model (C–H, 0.96 Å).

Conclusions

In summary, 3-phenyl-4-acyl-5-isoxazolones have proved to be highly efficient sensitizers for Tb^{3+} cation luminescence as demonstrated by the high emission quantum yields (59–72%) for luminescence which are up to three times as high as those reported previously for other *β*-diketonate ligands. This may be due to the superior match of the triplet energy level of the ligands with that of the Tb^{3+} emitting level. On the other hand, poor sensitization for Eu^{3+} has been noted for the above chromophores mainly due to the larger energy gap between the ligand triplet state and $^5D_0$ level of Eu^{3+}. Furthermore, in the present study, poly-*β*-hydroxybutyrate (PHB) polymer films doped with Tb^{3+}-3-phenyl-4-acyl-5-isoxazolonate complexes have been successfully prepared, characterized and investigated photophysical properties. The absence of the broad emission band of the PHB in doped systems indicated that the energy transfer *via* the polymer matrix to the Tb^{3+} is highly efficient, suggesting that the polymer matrix acts as a co-photoluminescent sensitizer. In addition, the higher quantum yields obtained for the doped PHB films (74–86%) as compared to hydrated Tb^{3+} complexes confirm the effect of sensitization induced by the polymer matrix. Furthermore, the influence of PHB on the coordinative environment of the Tb^{3+} ions changes the energy-transfer probabilities of the electric dipole transitions, accounting for the increases in luminescent intensity. In conclusion, the poly-*β*-hydroxybutyrate polymer films doped with Tb^{3+}-3-phenyl-4-acyl-5-isoxazolonate complexes are desirable for developing many applications in light conversion molecular devices.

Acknowledgements

The authors acknowledge financial support from the Department of Science and Technology (SR/S1/IC-36/20073), University Grants Commission and the Council of Scientific and

Industrial Research, New Delhi (NWP0023). A.H.C. thanks the Robert A. Welch Foundation (F-0003) for financial support. The authors also thank Dr Suresh Das, Head, Chemical Sciences & Technology Division, Mr Shinto Varghese and Dr Vidhya N., National Institute for Interdisciplinary Science & Technology (NIIST), Trivandrum, India, for their constant encouragement and valuable discussions. Dr Babu Varghese, Senior Scientific Officer, SAIF, IIT-Madras, is also acknowledged for X-ray crystallographic analysis.

References

1 (*a*) E. Brunet, O. Juanes and J. C. Rodriguez-Ubis, *Current Chemical Biology.*, 2007, **1**, 11; (*b*) D. Parker, J. A. G. Williams, *The Lanthanides and Their Interrelation with Biosystems*; M. Dekker, Inc.: New York, 2003, Vol. 40, p233.

2 (*a*) J.-C. G. Bünzli and C. Piguet, *Chem. Soc. Rev.*, 2005, **34**, 1048; (*b*) A. de Bettencourt-Dias, *Dalton Trans.*, 2007, 2229; (*c*) K. Kuriki, Y. Koike and Y. Okamoto, *Chem. Rev.*, 2002, **102**, 2347.

3 (*a*) J.-M. Lehn, *Angew. Chem. Int. Ed. Engl.*, 1990, **29**, 1304; (*b*) G. F. de Sa, O. L. Malta, C. de Mello Donega, A. M. Simas, R. L. Longo, P. A. Santa-Cruz and E. F. da Silva Jr., *Coord. Chem. Rev.*, 2000, **196**, 165; (*c*) D. B. Ambili Raj, S. Biju and M. L. P. Reddy, *Inorg. Chem.*, 2008, **47**, 8091.

4 (*a*) H. Xin, F. Y. Li, M. Shi, Z. Q. Bian and C. H. Huang, *J. Am. Chem. Soc.*, 2003, **125**, 7166; (*b*) M. Shi, F. Li, T. Yi, D. Zhang, H. Hu and C. Huang, *Inorg. Chem.*, 2005, **44**, 8929; (*c*) P. N. Remya, S. Biju, M. L. P. Reddy, A. H. Cowley and M. Findlater, *Inorg. Chem.*, 2008, **47**, 7396.

5 (*a*) S. Biju, D. B. Ambili Raj, M. L. P. Reddy and B. M. Kariuki, *Inorg. Chem.*, 2006, **45**, 10651; (*b*) S. Biju, M. L. P. Reddy and R. O. Freire, *Inorg. Chem. Commun.*, 2007, **10**, 393; (*c*) R. Pavithran, N. S. Saleesh Kumar, S. Biju, M. L. P. Reddy, S. Alves Jr. and R. O. Freire, *Inorg. Chem.*, 2006, **45**, 2184; (*d*) S. Biju, D. B. Ambili Raj, M. L. P. Reddy, C. K. Jayasankar, A. H. Cowley and M. Findlater, *J. Mater. Chem.*, 2009, **19**, 1425.

6 (*a*) J. Kai, D. F. Parra and H. F. Brito, *J. Mater. Chem.*, 2008, **18**, 4549; (*b*) Y. Hasegawa, M. Yamamuro, Y. Wada, N. Kanehisa, Y. Kai and S. Yanagida, *J. Phys. Chem. A*, 2003, **107**, 1697; (*c*) H. Liang, W. Wu, Y. Wang and Z. Li, *Spectrochim. Acta Part A*, 2005, **61**, 2687.

7 (*a*) L. D. Carlos, Y. Messaddeq, H. F. Brito, R. A. S. Ferreira, V. de Zea Bermudez and S. J. L. Ribeiro, *Adv. Mater.*, 2002, **12**, 594; (*b*) D. F. Parra, H. F. Brito, J. D. R. Matos and L. C. Dias, *J. Appl. Polym. Sci.*, 2002, **83**, 2716; (*c*) K. Binnemans, P. Lenaerts, K. Driesen and C. Gorller-Walrand, *J. Mater. Chem.*, 2004, **14**, 191; (*d*) L.-S. Fu, R. A. S. Ferreira, N. J. O. Silva, A. J. Fernandes, P. Ribeiro-Claro, I. S. Goncalves, V. de Zea Bermudez and L. D. Carlos, *J. Mater. Chem.*, 2005, **15**, 3117; (*e*) D. F. Parra, A. Mucciolo, D. G. Duarte, H. F. Brito and A. B. Lugao, *J. Appl. Polym. Sci.*, 2006, **100**, 406.

8 F. Korte and K. Storiko, *Ber. Dtsch. Chem. Ges.*, 1961, **94**, 1956.

9 P. Rabe, *Ber. Dtsch. Chem. Ges.*, 1897, **30**, 1614.

10 R. H. Prager, J. A. Smith, B. Weber and C. M. Williams, *J. Chem. Soc., Perkin Trans. 1*, 1997, 2659.

11 (*a*) N. Sabbatini, M. Guardigli and J.-M. Lehn, *Coord. Chem. Rev.*, 1993, **123**, 201; (*b*) V. Bekiari and P. Lianos, *Adv. Mater.*, 1998, **10**, 1455; (*c*) N. Sabbatini, A. Mecati, M. Guardigli, V. Balzani, J.-M. Lehn, R. Ziessel and R. Ungaro, *J. Lumin.*, 1991, **48–49**, 463; (*d*) K. Driesen, R. Van Deun, C. Gorller-Walrand and K. Binnemans, *Chem. Mater.*, 2004, **16**, 1531.

12 (*a*) L. N. Sun, J. B. Yu, G. L. Zheng, H. J. Zhang, Q. G. Meng, C. Y. Peng, L. S. Fu, F. Y. Liu and Y. N. Yu, *Eur. J. Inorg. Chem.*, 2006, **19**, 3962; (*b*) M. Kawa and J. M. J. Frechet, *Chem. Mater.*, 1998, **10**, 286; (*c*) H. R. Li, J. Lin, H. J. Zhang, L. S. Fu, Q. G. Meng and S. B. Wang, *Chem. Mater.*, 2002, **14**, 3651.

13 (*a*) M. Xiao and P. R. Selvin, *J. Am. Chem. Soc.*, 2001, **123**, 7067; (*b*) S. Comby, D. Imbert, C. Anne-Sophie, J.-C. G. Bünzli, L. J. Charvonniere and R. F. Ziessel, *Inorg. Chem.*, 2004, **43**, 7369.

14 (*a*) S. Viswanathan and A. de Bettenacourt-Dias, *Inorg. Chem.*, 2006, **45**, 10138; (*b*) Y. H. Kim, N. S. Baek and H. K. Kim, *ChemPhysChem*, 2006, **7**, 213.

15 I. Nasso, S. Bedel, C. Galaup and C. Picard, *Eur. J. Inorg. Chem.*, 2008, **12**, 2064.

16 (*a*) M. S. Wrighton, D. S. Ginley and D. L. Morse, *J. Phys. Chem.*, 1974, **78**, 2229; (*b*) J. C. de Mello, H. F. Wittmann and R. H. Friend, *Adv. Mater.*, 1997, **9**, 230.

17 T. Fiedler, M. Hilder, P. C. Junk, U. H. Kynast, M. M. Lezhnina and M. Warzala, *Eur. J. Inorg. Chem.*, 2007, **2**, 291.

18 (*a*) A. Dossing, *Eur. J. Inorg. Chem.*, 2005, **8**, 1425; (*b*) A. Beeby, I. M. Clarkson, R. S. Dickins, S. Faulkner, D. Parker, L. Royle, A. S. de Sousa, J. A. G. Williams and M. Woods, *J. Chem. Soc., Perkin Trans. 2*, 1999, 493.

19 S. V. Eliseeva, O. V. Kotova, F. Gumy, S. N. Semenov, V. G. Kessler, L. S. Lepnev, J.-C. G. Bünzli and N. P. Kuzmina, *J. Phys. Chem. A*, 2008, **112**, 3614.

20 A. P. S. Samuel, E. G. Moore, M. Melchior, J. Xu and K. N. Raymond, *Inorg. Chem.*, 2008, **47**, 7535–7544.

21 F. J. Steemers, W. Verboom, D. N. Reinhoudt, E. B. van der Tol and J. W. Verhoeven, *J. Am. Chem. Soc.*, 1995, **117**, 9408.

22 M. Latva, H. Takalo, V.-M. Mukkala, C. Matachescu, J. C. Rodriguez-Ubis and J. Kankare, *J. Lumin.*, 1997, **75**, 149.

23 (*a*) D. F. Parra, A. Muccicolo and H. F. Brito, *J. Appl. Polym. Sci.*, 2004, **94**, 865; (*b*) Q. Li, T. Li and J. Wu, *J. phys. Chem. B*, 2001, **105**, 12293.

24 J.-C. G. Bunzli, Luminescent Probes. In *Lanthanide Probes in Life, Chemical and Earth Sciences, Theory and Practice*; Bunzli, J.-C. G., Choppin, G. R., Eds.; Elsevier: New York, 1989; p 219.

25 G. Linger, R. Mohan, S. Knittel and G. Duportail, *Spectrochim. Acta*, 1990, **464**, 797.

26 A. F. Kirby, D. Foster and F. S. Richardson, *Chem. Phys. Lett.*, 1983, **95**, 507.

27 N. S. Poluektov, V. N. Drobyazko, S. B. Meshkova, S. L. Bel'tyukova and L. I. Kononenko, *Dokl. Akad. Nauk., SSSR 224*, 1975, 150.

28 (*a*) L.-O. Pålsson and A. P. Monkman, *Adv. Mater.*, 2002, **14**, 757; (*b*) B. K. Shah, D. C. Neckers, J. Shi, E. W. Forsythe and D. Morton, *Chem. Mater.*, 2006, **18**, 603.

29 (*a*) M. Cölle, J. Gmeiner, W. Milius, H. Hillebrecht and W. Brütting, *Adv. Funct. Mater.*, 2003, **13**, 108; (*b*) N. S. Saleesh Kumar, S. Varghese, N. P. Rath and S. Das, *J. Phys. Chem. C*, 2008, **112**, 8429.

30 G. M. Sheldrick, *SHELXL-PC*, version 5; Siemens Analytical X-ray Instruments. Inc.: Madison, WI, USA, 1994.